Cupric oxide as an induced-multiferroic with high-T_C

T. KIMURA[1]*, Y. SEKIO[1], H. NAKAMURA[1], T. SIEGRIST[2] AND A. P. RAMIREZ[2]

[1]Division of Materials Physics, Graduate School of Engineering Science, Osaka University, Toyonaka, Osaka 560-8531, Japan
[2]Bell Laboratories, Alcatel-Lucent, 600 Mountain Avenue, Murray Hill, New Jersey 07974, USA
*e-mail: kimura@mp.es.osaka-u.ac.jp

Materials that combine coupled electric and magnetic dipole order are termed 'magnetoelectric multiferroics'[1–4]. In the past few years, a new class of such materials, 'induced-multiferroics', has been discovered[5,6], wherein non-collinear spiral magnetic order breaks inversion symmetry, thus inducing ferroelectricity[7–9]. Spiral magnetic order often arises from the existence of competing magnetic interactions that reduce the ordering temperature of a more conventional collinear phase[10]. Hence, spiral-phase-induced ferroelectricity tends to exist only at temperatures lower than ∼40 K. Here, we propose that copper(II) oxides (containing Cu^{2+} ions) having large magnetic superexchange interactions[11] can be good candidates for induced-multiferroics with high Curie temperature (T_C). In fact, we demonstrate ferroelectricity with $T_C = 230$ K in cupric oxide, CuO (tenorite), which is known as a starting material for the synthesis of high-T_c (critical temperature) superconductors. Our result provides an important contribution to the search for high-temperature magnetoelectric multiferroics.

Since the discovery of high-critical-temperature (T_c) superconductivity in cuprates, the magnetic superexchange interaction between nominally divalent copper ions coordinated by oxygen in low-dimensional cuprates has been extensively studied. The magnitude and the sign of the principal superexchange interaction J in the low-dimensional cuprates strongly depend on crystallographic structural parameters. Recently, Shimizu and co-workers pointed out a systematic correlation between J and the Cu–O–Cu bond angle ϕ in low-dimensional cuprates[12]. In Fig. 1, J is plotted against ϕ for various low-dimensional cuprates including parent compounds of high-T_c superconductors[12–16]. As seen in Fig. 1, J is of the order of 10^2 meV in parent compounds of high-T_c superconductors with $\phi \sim 180°$ (ref. 11), which is much greater than that in most ionic antiferromagnets where ϕ is less than $180°$ and typical J values are less than 10 meV. In addition, the compounds having large J show high Néel temperatures (T_N) in the vicinity of room temperature. With decreasing ϕ, J is monotonically suppressed and eventually becomes negative (ferromagnetic) at around $\phi = 95°$. As a result, the ferromagnetic J competes with higher-order superexchange interactions, often leading to spiral magnetic order in cuprates with small ϕ. In addition, ferroelectricity induced by spiral magnetic order has recently been observed in $LiCu_2O_2$ and $LiCuVO_4$ (refs 17,18). However, both their magnetic and ferroelectric ordering temperatures are lower than 25 K. Figure 1 provides a useful guide to develop induced-multiferroics with high ferroelectric Curie temperature (T_C). If we can fine-tune ϕ
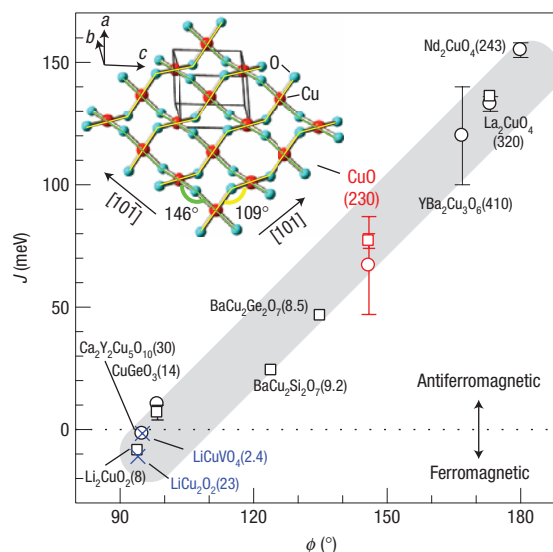

Figure 1 Principal superexchange interaction J as a function of Cu–O–Cu bond angle ϕ for various low-dimensional cuprates. CuO (red) has an intermediate magnitude of J among the various cuprates. The plot of J versus ϕ for cuprates was originally presented in refs 12,13. (Open circles and crosses represent the data obtained from neutron scattering. Open squares are the data obtained from susceptibility measurements.) $LiCu_2O_2$ and $LiCuVO_4$ (blue) show ferroelectricity induced by spiral magnetic order. Figures in parentheses denote magnetic ordering temperatures of the respective compounds. The inset shows a schematic diagram of the crystal structure of CuO. The Cu–O zigzag chains run along the [101] (yellow lines) and the [10$\bar{1}$] (green lines) directions. Only Cu atoms with the same b coordinate are shown. The grey line is a guide to the eyes.

in a low-dimensional cuprate, we can simultaneously achieve spiral magnetic order with a high ordering temperature and, consequently, a magnetically induced ferroelectric state at temperatures much higher than reported previously. To examine this prediction, we investigated the electric properties of CuO (tenorite).

The $C2/c$ monoclinic crystal structure of CuO is unique among $3d$ transition-metal monoxides in departing considerably from the simple NaCl-type structure[19]. The structure of CuO can be viewed as being composed from two types of zigzag Cu–O chains running
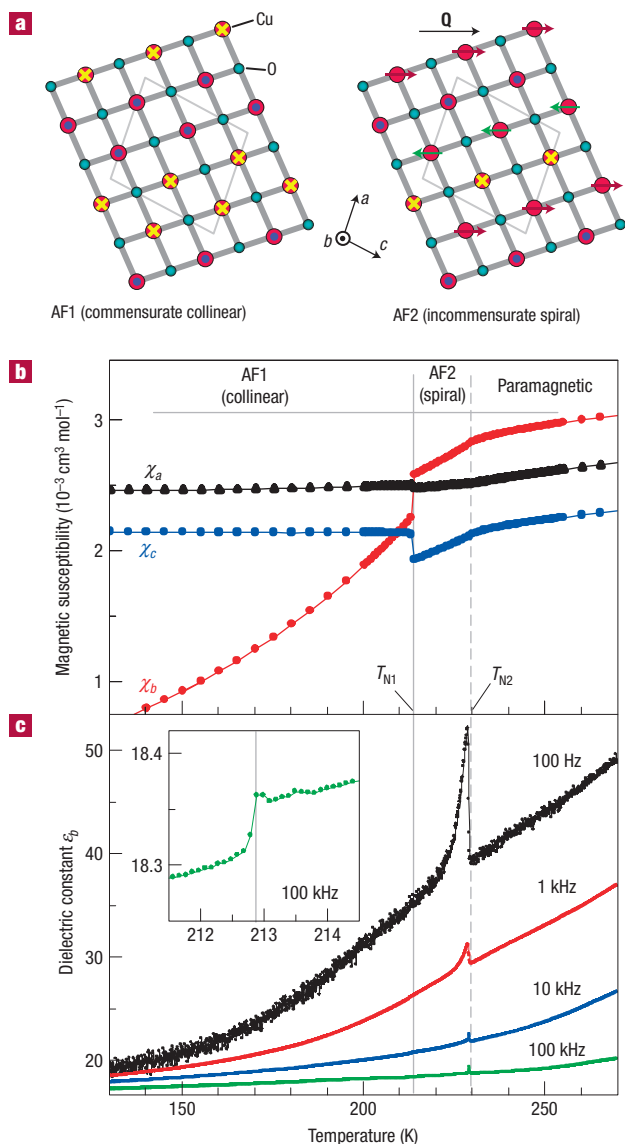
AF1 (commensurate collinear)   AF2 (incommensurate spiral)

Figure 2 Dielectric anomalies at magnetic phase transitions in CuO.
a, Schematic illustrations of the magnetic structures in the commensurate collinear AF1 (left panel) and the incommensurate spiral AF2 (right panel) phases. Red and green arrows, yellow crosses and dark-blue circles denote Cu magnetic moments. **b**, Temperature profiles of magnetic susceptibility measured along the reciprocal lattice axes. **c**, Temperature profiles of dielectric constant measured along the b^* axis (ε_b) at selected frequencies. The inset shows a magnified view of ε_b at 100 kHz around T_{N1}.

along the [10$\bar{1}$] and [101] directions (see the inset of Fig. 1). Here, ϕ is 146° in the [10$\bar{1}$] chains and 109° in the [101] chains, which makes J along the [10$\bar{1}$] chain the dominant interaction. It might be expected that an angle of 146° being intermediate between 90° and 180° would produce spiral order arising from the competing antiferromagnetic and ferromagnetic interactions, while maintaining a high effective J. In fact, J along [10$\bar{1}$] chains in CuO is 60–80 meV (refs 12,20), which is similar to that in parent compounds of high-T_c cuprates. CuO undergoes two successive magnetic transitions at $T_{N1} = 213$ K and $T_{N2} = 230$ K (refs 20,21). Such a high T_N can naturally be ascribed to the strong J. In addition, an incommensurate spiral magnetic structure, the AF2

phase, shows up between T_{N1} and T_{N2}. The right panel of Fig. 2a shows a rough sketch of the magnetic structure model proposed on the basis of polarized neutron diffraction studies[22,23]. Below T_{N2}, in the AF1 phase, the magnetic moments are aligned collinearly along b and order antiferromagnetically along the [10$\bar{1}$] chains and ferromagnetically along the [101] chains, as shown in the left panel of Fig. 2a.

Figure 2b shows the temperature profiles of the magnetic susceptibility for the reciprocal lattice axes (χ_a, χ_b and χ_c for a^*, b^* and c^*, respectively) of a single crystal of CuO. On cooling, χ_b shows a kink at T_{N2} and a discontinuous drop at T_{N1}, whereas χ_c exhibits a kink at T_{N2} and a discontinuous jump at T_{N1}. The observed anomalies are similar to those reported previously[24]. Measurements of the dielectric constant ε revealed that the magnetic transitions affect the dielectric properties. Figure 2c shows the temperature dependence of ε along the b^* (or b) axis (ε_b) at several frequencies for a CuO crystal. The temperature dependence of ε_b at all the frequencies exhibits a sharp peak structure at $T_{N2} = 230$ K, which suggests a ferroelectric transition. In addition, a smaller stepwise anomaly appears at T_{N1}, as shown in the inset of Fig. 2c. Although we also carried out measurements of ε_a and ε_c, dielectric anomalies at T_{N1} and T_{N2} were observed only in ε_b.

In previous studies, CuO is discussed as a charge-transfer insulator[25], becoming conductive owing to holes arising from the presence of a microscopically small quantity of Cu^{3+} (ref. 26). As expected, the previously reported dielectric constant of CuO showed a striking sample dependence from highly insulating with $\varepsilon = 10^0$–10^1 to semiconducting with $\varepsilon = 10^3$–10^4 samples[27,28]. Therefore, the large difference in ε for CuO has been interpreted in terms of the difference in the density of Cu^{3+} impurities. A relatively small magnitude of ε ($\sim10^1$) in the present sample suggests a small density of Cu^{3+}. Although the temperature dependence of ε for both polycrystalline and single-crystal samples of CuO was reported previously[27,28], the focus was only on the large dielectric constants ($\varepsilon = 10^3$–10^4) in semiconducting samples and in directions other than b^*. Thus, the data shown in Fig. 2c are the first observation of the sharp peak structure in ε at T_{N2}.

Figure 3 shows the temperature profiles of the electric polarization along the b^* (or b) axis (P_b) obtained from measurements of the pyroelectric current. For these measurements, the sample was cooled down while applying a poling electric field ($+117$ or -117 kV m^{-1}). At 220 K, the poling electric field was removed. Then, the pyroelectric current was measured during cooling or heating the sample. No substantial electric polarization (P) exists below T_{N1} and above T_{N2}, whereas a finite P shows up between T_{N1} and T_{N2}. These results clearly indicate that only the non-collinear spiral AF2 phase is polar in CuO. In addition, the polarity can be switched by the sign of the poling electric fields, which suggests ferroelectricity in the AF2 phase (compare black and grey data in Fig. 3).

To confirm that the AF2 phase is ferroelectric, we need to demonstrate reversal of the spontaneous polarization by an external electric field E. Despite the sample being insulating, the conventional Sawyer–Tower method could not be used owing to larger leakage currents. Although ref. 27 reported P–E hysteresis loops in a semiconductive CuO crystal with E along the c axis from $90 < T < 250$ K, the loop feature seems to be attributed to dielectric loss. To overcome this problem, we carried out the following experiment. First, the sample was poled by applying a positive (or negative) E above T_{N2}, and was cooled down to 220 K (AF2 phase). After the poling procedure, the E was turned off. Subsequently, we applied an opposite (or zero) electric field (E_{rev}) to the poling E. Then, we carried out pyroelectric measurements at $E = 0$, and obtained the temperature profiles of
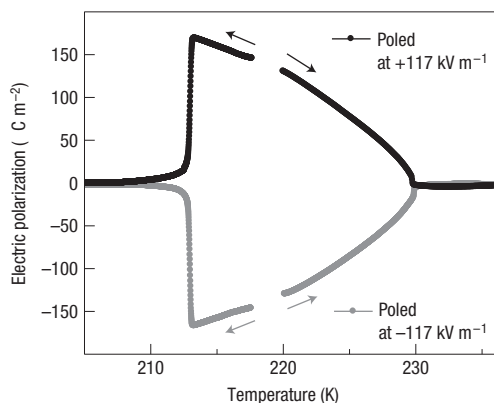
Figure 3 Electric polarization along the b^* axis as a function of temperature for a CuO crystal. To pole the crystal, electric fields of $+117$ and $-117\,\mathrm{kV\,m^{-1}}$ were applied above T_{N2} for the data denoted by black and grey circles, respectively, and then the crystal was cooled to the lower boundary of the AF2 phase (220 K). After these procedures, the poling electric fields were removed, and the pyroelectric current was measured during the temperature up and down sweeps. Arrows indicate the direction of the temperature sweep during the respective measurements.

P_b shown in Fig. 4b,c. In Fig. 4b,c, the sign of P_b is reversed when $|E_{rev}| > {\sim}55\,\mathrm{kV\,m^{-1}}$ was applied. These results demonstrate that the spontaneous polarization can be reversed by E and the coercive field at 220 K is around ${\sim}55\,\mathrm{kV\,m^{-1}}$. By plotting the value of P_b at 220 K of the respective E_{rev} data, we can draw a P–E hysteresis loop, as shown in Fig. 4a. Thus, we confirmed that the AF2 phase is ferroelectric. The maximum value of P in CuO is of the order of $10^2\,\mathrm{\mu C\,m^{-2}}$, which is comparable to most of the known induced-multiferroics[6]. We emphasize, however, that T_C of CuO (230 K) is much higher than any of them (<40 K).

In the past few years, it has been widely accepted that ferroelectricity can appear owing to a cycloidal spiral magnetic order in which the plane of the spiral is parallel to the magnetic modulation vector $\mathbf{Q}$ (refs 5–8). According to this cycloidal scenario, the direction of P is in the spiral plane and perpendicular to $\mathbf{Q}$. In CuO, if we consider the incommensurate magnetic structure in the AF2 phase ($\mathbf{q}_2 = (0.506, 0, -0.483)$) as a modulated structure with a little larger period of the commensurate AF1 state ($\mathbf{q}_1 = (1/2, 0, -1/2)$) (ref. 23), the modulation vector $\mathbf{Q}$ in the incommensurate spiral AF2 phase is expressed as $\mathbf{Q} = \mathbf{q}_2 - \mathbf{q}_1 = (0.006, 0, 0.017)$. The plane of the spiral is parallel to $\mathbf{b}^*$ and $\mathbf{v} = 0.506\mathbf{a}^* + 1.517\mathbf{c}^*$ (ref. 23), where $\mathbf{v}$ is almost parallel to $\mathbf{Q}$. This indicates that the magnetic structure in the AF2 phase can be regarded as a cycloidal spiral. The expected direction of P in the AF2 phase by the cycloidal scenario[5–8] is along b, which is consistent with our experimental result.

Considering the monoclinic structure (point group; $2/m$) of CuO, we may also apply another explanation proposed by Arima[9] for explaining the ferroelectricity in CuO. He pointed out the possibility of ferroelectricity in monoclinic crystals with a proper-screw spiral magnetic order in which the spiral plane is perpendicular to $\mathbf{Q}$ (ref. 9). In monoclinic CuO with a nonpolar point group $2/m$, spiral magnetic order with $\mathbf{Q}$ normal to the two-fold rotation axis ($\parallel b$) removes the (glide) mirror plane perpendicular to the two-fold rotation axis, and makes the system a polar point group 2. The observed P along b ($\perp$ removed mirror plane) in the AF2 phase also agrees well with the expected direction of P by this explanation.

The present result provides a new route to develop induced-multiferroics with high-T_C, that is, use of low-dimensional cuprates
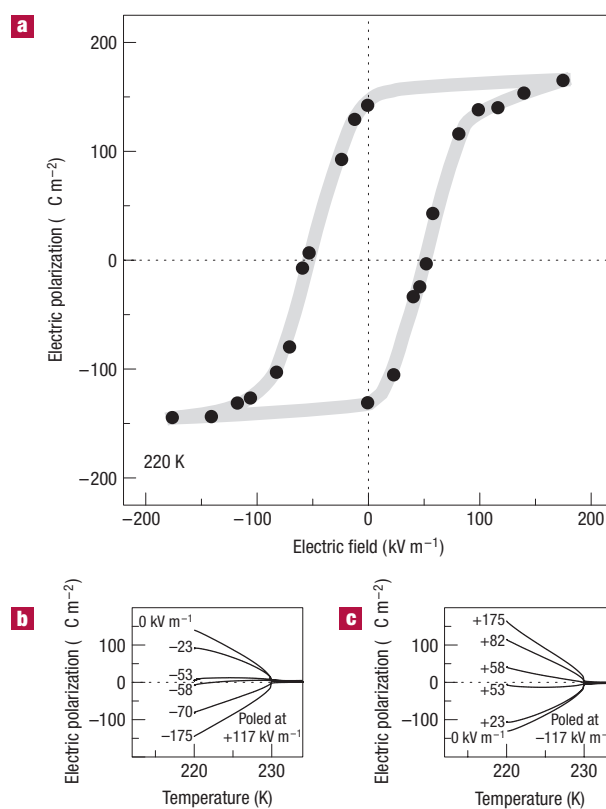

Figure 4 Electric polarization hysteresis in CuO. a, Electric polarization as a function of electric fields applied along the b^* axis at 220 K for a CuO crystal. **b,c**, Electric polarization as a function of temperature. Before the measurements, electric fields of $+117$ and $-117\,\mathrm{kV\,m^{-1}}$ were applied above T_{N2} for the data shown in **b** and **c**, respectively, and then the crystal was cooled down to the lower boundary to the AF2 phase (220 K). The respective measurements in **b** and **c** were done in the absence of applied electric fields after an opposite (or zero) poling electric field was applied for a while at 220 K. The data points in **a** were taken from the data at 220 K of the respective P–T curves in **b** and **c**. Grey line in **a** is a guide to the eyes.

with large superexchange interactions. Another aspect for the present finding is that a new ferroelectric compound, CuO, can be a rare example of a binary ferroelectric compound. Although many ferroelectrics have been reported so far, most of them are composed of more than three elements and only a few binary compounds (for example, HCl and HBr (ref. 29)) have been proven as ferroelectrics.

METHODS

We have grown single crystals of CuO under ${\sim}8$ atm of pure oxygen by the floating zone technique, following ref. 30. The grown crystals were characterized by powder X-ray diffraction measurements confirming the $C2/c$ monoclinic structure ($a = 4.68$ Å, $b = 3.42$ Å, $c = 5.129$ Å, and $\beta = 99.54°$) at room temperature. The crystals were oriented using X-ray diffractometers, and cut into thin plates with the widest faces perpendicular to the crystallographic principal axes. The magnetic susceptibility of the crystals was measured with a commercial magnetometer at the Low Temperature Center at Osaka University. For the measurements of dielectric constant and pyroelectric current, silver electrodes were sputtered onto the widest faces of the samples. The dielectric constant was measured over a range of frequencies using an LCR (inductance–capacitance–resistance) meter. The electric polarization was obtained from integration of the pyroelectric current by time. We also carried out measurements of the resistivity ρ. The resistivity shows a highly insulating feature ($\rho_{\parallel b} = 10^6$–$10^7$ Ω cm in the AF2 phase) and does not show any anomalies at the magnetic transition temperatures.

LETTERS

References

1. Hill, N. A. Why are there so few magnetic ferroelectrics? *J. Phys. Chem. B* **104**, 6694–6709 (2000).
2. Fiebig, M. Revival of the magnetoelectric effect. *J. Phys. D* **38**, R123–R152 (2005).
3. Khomskii, D. I. Multiferroics: Different ways to combine magnetism and ferroelectricity. *J. Magn. Magn. Mater.* **306**, 1–8 (2006).
4. Eerenstein, W., Mathur, N. D. & Scott, J. F. Multiferroic and magnetoelectric materials. *Nature* **442**, 759–765 (2006).
5. Cheong, S.-W. & Mostovoy, M. V. Multiferroics: A magnetic twist for ferroelectricity. *Nature Mater.* **6**, 13–20 (2007).
6. Kimura, T. Spiral magnets as magnetoelectrics. *Annu. Rev. Mater. Res.* **37**, 387–413 (2007).
7. Katsura, H., Nagaosa, N. & Balatsky, A. V. Spin current and magnetoelectric effect in noncollinear magnets. *Phys. Rev. Lett.* **95**, 057205 (2005).
8. Kenzelmann, M. *et al.* Magnetic inversion symmetry breaking and ferroelectricity in $TbMnO_3$. *Phys. Rev. Lett.* **95**, 087206 (2005).
9. Arima, T. Ferroelectricity induced by proper-screw type magnetic order. *J. Phys. Soc. Japan* **76**, 073702 (2007).
10. Ramirez, A. P. Strongly geometrically frustrated magnets. *Annu. Rev. Mater. Sci.* **24**, 453–480 (1994).
11. Kastner, M. A., Birgeneau, R. J., Shirane, G. & Endoh, Y. Magnetic, transport, and optical properties of monolayer copper oxides. *Rev. Mod. Phys.* **70**, 897–928 (1998).
12. Shizmizu, T., Matsumoto, T., Goto, T., Yoshimura, K. & Kosuge, K. Magnetic dimensionality of the antiferromagnet CuO. *J. Phys. Soc. Japan* **72**, 2165–2168 (2003).
13. Mizuno, Y. *et al.* Electronic states and magnetic properties of edge-sharing Cu–O chains. *Phys. Rev. B* **57**, 5326–5334 (1998).
14. Tsukada, I. *et al.* $BaCu_2Si_2O_7$: A quasi-one-dimensional $S = 1/2$ antiferromagnetic chain system. *Phys. Rev. B* **60**, 6601–6607 (1999).
15. Masuda, T. *et al.* Spin waves and magnetic interactions in $LiCu_2O_2$. *Phys. Rev. B* **72**, 014405 (2005).
16. Enderle, M. *et al.* Quantum helimagnetism of the frustrated spin-1/2 chain $LiCuVO_4$. *Europhys. Lett.* **70**, 237–243 (2005).
17. Park, S., Choi, Y. J., Zhang, C. L. & Cheong, S.-W. Ferroelectricity in an $S = 1/2$ chain cuprates. *Phys. Rev. Lett.* **98**, 057601 (2007).
18. Naito, Y. *et al.* Ferroelectric transition induced by the incommensurate magnetic ordering in $LiCuVO_4$. *J. Phys. Soc. Japan* **76**, 023708 (2007).
19. Åsbrink, S. & Norrby, L.-J. A refinement of crystal structure of copper(II) oxide with a discussion of some exceptional e.s.d.'s. *Acta Crystallogr. B* **26**, 8–15 (1970).
20. Yang, B. X., Thurston, T. R., Tranquada, J. M. & Shirane, G. Magnetic neutron scattering study of single-crystal cupric oxide. *Phys. Rev. B* **39**, 4343–4349 (1989).
21. Forsyth, J. B., Brown, P. J. & Wanklyn, B. M. Magnetism in cupric oxide. *J. Phys. C* **21**, 2917–2929 (1989).
22. Brown, P. J., Chattopadhyay, T., Forsyth, J. B., Nunez, V. & Tasset, F. Antiferromagnetism in CuO studied by neutron polarimetry. *J. Phys. Condens. Matter* **3**, 4281–4287 (1991).
23. Ain, M., Menelle, A., Wanklyn, B. M. & Bertaut, E. F. Magnetic structure of CuO by neutron diffraction with polarization analysis. *J. Phys. Condens. Matter* **4**, 5327–5338 (1992).
24. Köbler, U. & Chattopadhyay, T. On the magnetic anisotropy of CuO. *Z. Phys. B* **82**, 383–386 (1991).
25. Ghisen, J. *et al.* Electronic-structure of Cu_2O and CuO. *Phys. Rev. B* **38**, 11322–11330 (1988).
26. Collins, B. T., DeSisto, W., Kershaw, R., Dwight, K. & Wold, A. Preparation and characterization of Cu(II) oxide. *J. Less-Common Met.* **156**, 341–346 (1989).
27. Zheng, X. G. *et al.* Dielectric measurement to probe electron ordering and electron–spin interaction. *J. Appl. Phys.* **92**, 2703–2708 (2002).
28. Sarkar, S., Kumar, J. P. K., Chaudhuri, B. K. & Sakata, H. Copper(II) oxide as giant dielectric material. *Appl. Phys. Lett.* **89**, 212905 (2006).
29. Hoshino, S., Shimaoka, K. & Niimura, N. Ferroelectricity in solid hydrogen halides. *Phys. Rev. Lett.* **19**, 1286–1288 (1967).
30. Prabhakaran, D. & Boothroyd, A. T. Single crystal growth of Zn-doped CuO by the floating zone method. *J. Cryst. Growth* **250**, 77–82 (2003).